Improvement of mechanical and optical properties of Na2O–CaO–SiO2 glasses based on dune sand

Siham Aissou, Nedjima Bouzidi, Laurent Cormier, Eduardo Bonet-Martinez, Djoudi Merabet

BOLETIN DE LA SOCIEDAD ESPAÑOLA DE
Cerámica y Vidrio
www.elsevier.es/bsecv

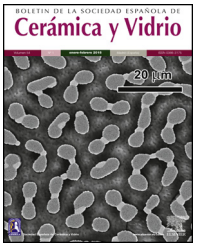

Improvement of mechanical and optical properties of Na_2O–CaO–SiO_2 glasses based on dune sand

Siham Aissou[a,*], *Nedjima Bouzidi*[a], *Laurent Cormier*[b], *Eduardo Bonet-Martinez*[c], *Djoudi Merabet*[a]

[a] *Laboratoire de Technologie des Matériaux du Génie des Procédés (LTMGP), Département de Génie des procédés, Faculté Technologie, Université de Bejaia, Route de Targa Ouzemour, 06000 Bejaia, Algeria*
[b] *Sorbonne Université, CNRS, MNHN, IRD, Institut de Minéralogie, de Physique des Matériaux et de Cosmochimie (IMPMC), 4 place Jussieu, F-75005 Paris, France*
[c] *Department of Chemical, Environmental, and Materials Engineering. University of Jaen, Campus Las Lagunillas, s/n, 23071 Jaén, Spain*

ARTICLE INFO

Article history:
Received 10 January 2018
Accepted 22 May 2018
Available online 2 July 2018

Keywords:
Dune sand
Glass
Color
Knoop Microhardness
Chemical durability

ABSTRACT

This work aims to discuss on the characterization of Algerian dune sand named Boussaâda sand (S_B) and its suitability for glass industry. Based on chemical and mineralogical analyses of S_B by XRF and XRD, quartz, kaolinite, calcium carbonates and albite are the main mineralogical phases found. However, Fe_2O_3 content is relatively low (<0.24 wt%). Optical properties of the elaborated glass determined by UV-Visible Spectroscopy reveal that S_B based glass (G_B) presents better light transmission than industrial used sand (S_T) based glass (G_T). The CIE L*a*b* color measurements show that the sample is colorless. Knoop Hardness measurements indicate that G_T is more hard than G_B. Chemical durability tests reveal that in an acid solution, G_B is more resistant, whereas it is more vulnerable in the presence of alkaline and HF solution. Furthermore, TiO_2 additions in S_B-based glass improve the clarity and transparency of the glasses (from $L^* = 87.67$ to $L^* = 91.05$ with 1 wt% of TiO_2). Thus, when TiO_2 content increased, Knoop microhardness enhance (from 451 to 469 HK with 0.1 wt% of TiO_2). An increase in the glass chemical durability of the samples in acidic and alkaline solutions is noticed when trace amounts of TiO_2 are added to the glass.

Mejora de los propiedades mecánicas y ópticas de los vidrios de Na_2O-CaO-SiO_2 basados en arena de duna

Palabras clave:
Arena de duna
Vidrio
Color
Microdureza Knoop
Durabilidad química

RESUMEN

Este trabajo tiene como objetivo la caracterización de arena de duna Argelina llamada arena Boussaâda (S_B) y su idoneidad para la industria del vidrio. Basado en análisis químicos y mineralógicos de S_B por XRF y XRD, cuarzo, caolinita, carbonatos de calcio y albita fueron las principales fases mineralógicas encontradas. Sin embargo, el contenido de Fe_2O_3 es relativamente bajo (<0.24% en peso). Las propiedades ópticas del vidrio elaborado determinadas por espectroscopia UV-Visible. Este parámetro revela que el vidrio a base de S_B (G_B) presenta

* *Corresponding author.*
E-mail address: aissousiham@yahoo.fr (S. Aissou).
https://doi.org/10.1016/j.bsecv.2018.05.002

una mejor transmisión de luz que el vidrio industrial a base de arena (S_T) y de vidrio (G_T). Las mediciones de color CIE L*a*b* muestran que la muestra es incolora. Las mediciones de dureza Knoop indican que G_T es más duro que G_B. Las pruebas de durabilidad química revelan que en solución ácida, G_B es más resistente, mientras que es más vulnerable en presencia de soluciones alcalinas y de HF. Las adiciones de TiO_2 al vidrio a base de S_B mejoran la claridad y transparencia de los vidrios (de $L^* = 87.67$ a $L^* = 91.05$ con 1% en peso de TiO_2). Además, se observó un aumento de la durabilidad química de las muestras en solución ácida y alcalina cuando se añadieron cantidades de TiO_2.

Introduction

Algeria possesses large deposits of siliceous raw materials, particularly in the west of the country, where they are linked to the deposits of wind sands. It is mainly these deposits that are exploited for the glass production. These potential resources of siliceous materials are very important because of their distribution, extension and diversity [1].

The Tebessa-treated silica sand, East of Algeria, is exploited as raw material in flat glass industry. However, the demand for this raw material is important that the glass companies are forced to import it from abroad, especially from France (Fontainebleau) to satisfy the demand.

Several research projects valuing Algerian dune sands in the field of construction are carried out in the recent years. Therefore, the development of insulating materials based on Ouargla's sand [2] and the valorization of Djelfa and Boussaâda sands in Cement industry to improve the performance of concrete were the only applications of these sands [3–5]. However, investments in these siliceous natural resources are below expected levels due to the lack of detailed studies on their physicochemical characterization [6], which limits developers to focus on the exploitation of these siliceous sands in glass industry and to provide solutions to the problems of sand supply.

The silica content and the particle size distribution are not the only criteria for the suitability of sands for the glass industry. Most of the time, silica contains trace metallic impurities which affect the process of production as well as the properties of the elaborated glasses [7–9]. One of the most common and undesirable impurity is iron either in ferrous (Fe^{2+}) or ferric (Fe^{3+}) state. This impurity dramatically influences the optical, colorimetric and mechanical properties of glasses [10,11]. Besides, the presence of alumina (clay fraction) yields devitrification phenomena in the glasses. Innumerable researches have been carried out to optimize and improve processes for purification and treatment of sands such as attrition, flotation, washing and magnetic separation [12–14]. Another alternative or complementary operation to these purification processes is carried out at the level of the glass formulations and this by adding small amounts of transitions metal oxides which influence the red/ox state of the iron impurity thus eliminating their undesirable effects on the glasses colorimetric and optical properties [15]. For example, TiO_2 addition in small amounts to the glass composition influences the equilibrium of the Fe^{3+}/Fe^{2+}, leading to an improvement in the colorimetric and optical properties of glasses [10,16]. This addition also influences the mechanical and thermo-mechanical properties of glasses by reinforcing the vitreous matrix [10,17,18]. TiO_2 containing glasses also possess good chemical durability to acid attack [19].

From this perspective, this work deals with the characterization of the dune sand of Boussaâda located in South East of Algeria. Its valorization in the development of soda-lime-silica glasses is the first objective of this work. An attempt to improve the colorimetric, optical and chemical durability of the glasses produced by adding TiO_2 at variable amounts to the glass compositions is the second objective of this work. For these purposes six glass compositions with and without TiO_2 addition are prepared. They are denoted G_{Bx}, with $x = 1$, 2, 4, 6 and 10 corresponding to 0.1, 0.2, 0.4, 0.6 and 1 wt% of TiO_2 added, respectively. One sample (G_T) with Tebessa sand, used in local glass industry, is also prepared for comparison.

Experimental part

Raw materials

The local materials used in this work are: The dune sand of Boussaâda (S_B), Tebessa sand (S_T) usually used in the glass industry and natural dolomite (D) [$MgCa(CO_3)_2$].

The S_B sand is a sample taken in the area situated in the Boussaâda dune cordon. This area is part of the Zahrez Gharbi basin in the high south of Algeria [20]. The dune cordon is a recent geological formation which appears in the end of tertiary and the beginning of the quaternary. It is coming from the soft rocks (marlstone and red clay) which have been extracted by the erosion of the mountain as well as the presence of the salt Limestone, Gypsum and soluble salts [20].

Treatment of Boussaâda sand

Before the preparation of the samples (glass), S_B sand is washed several times with distilled water for removing the fine fraction. Then it is dried in ambient air, sieved to a particle size greater than 100 μm and ground.

Table 1 – Proportion of raw materials in the samples (wt%).

Components	Sand	$CaCO_3$	Na_2CO_3	Na_2SO_4	$MgCa(CO_3)_2$	TiO_2
Proportion, wt%	61.29-x	14.36	19.85	0.5	4	x = 0, 0.1, 0.2, 0.4,0.6 or 1

Glasses Elaboration

The basic glass compositions are summarized in Table 1. A homogenized mixture of 40 g of raw materials: sand, dolomite and chemical reagents (Na_2CO_3, $CaCO_3$ and Na_2SO_4 from Cheminova International, Spain with a chemical purity of 99 wt%) is placed in a platinum crucible in an electric furnace for a calcination step at 850 °C for 6 h, followed by a first melting step for 2 h at 1450 °C. The glass obtained by quenching is ground to increase homogeneity. This stage is followed by a second melting step at 1450 °C for 4 h, followed by annealing at 560 °C for a period of one hour. The samples are cut into test tubes, polishing (P400, P600, P1200, P2500, P40000 and with diamond paste) and grinding until obtaining a powder with a particle size ≤ 0.63 mm. The experimental procedure of the obtained materials is presented in Fig. 1.

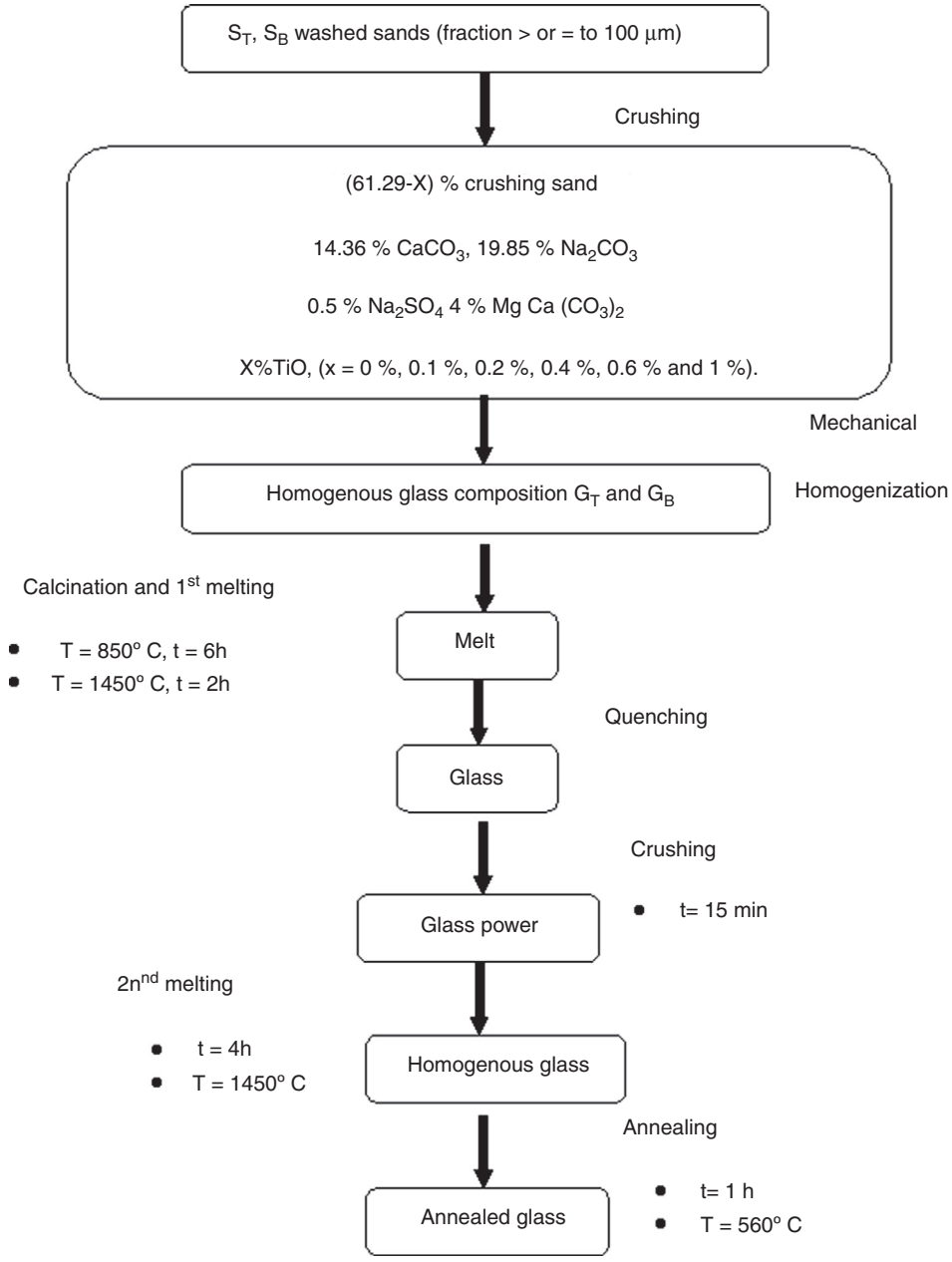

Fig. 1 – Diagram of the experimental procedure of the obtained glasses.

Table 2 – Chemical composition of raw materials.

Sand	Oxides	SiO_2	Al_2O_3	CaO	Fe_2O_3	MgO	Na_2O	K_2O	TiO_2	L.O.I
S_B	wt%	95.21 ± 0.01	0.97 ± 0.03	1.32 ± 0.02	0.23 ± 0.02	0.01 ± 0.03	0.27 ± 0.02	0.40 ± 0.04	0.01 ± 0.004	1.52 ± 0.01
S_T	wt%	98.20 ± 0.01	0.88 ± 0.03	0.20 ± 0.02	0.12 ± 0.02	0.05 ± 0.03	0.05 ± 0.02	0.34 ± 0.04	0.07 ± 0.004	0.09 ± 0.01
D	wt%	0.48 ± 0.01	0.36 ± 0.02	30.77 ± 0.01	0.06 ± 0.02	21.00 ± 0.03	n.d	n.d	n.d	47.42 ± 0.01

L.O.I: Loss On Ignition, n.d: not determined.

Improvement of the glasses properties

With the aim to improving the color and chemical durability of S_B glasses, several glasses were elaborated based on TiO_2 addition. They are elaborated using the same procedure: two melting steps and in the same conditions of temperature and time (Table 1 and Fig. 1).

Characterization of the raw materials and the elaborated glasses

The mineralogical compositions of the two sands were determined used an X-ray PANalytical X' Pert PRO diffractometer (Cu Kα, λ = 1.540598 Å, 2θ range 0–80°, 0.025 2θ step). The collected data are processed by PANalytical X' Pert Highscore software.

The Thermo gravimetric and Differential Thermal sand analyses were carried out using a NETZSCH STA 409 C/CD thermo balance allowing the two analyzes to be coupled during the same thermal cycle. The TGA/DTA curves are obtained using a rate of 10 °C/min from room temperature to 1000 °C. The samples, about 300 mg, are placed in alumina crucible under argon atmosphere.

The S_B Sand particle size distribution was realized using a MASTERSIZER 2000 Laser granulometer.

The chemical composition of S_B, S_T Sands and dolomite (Table 2) were carried out by X-ray fluorescence (PANalytical Perl'X 3). The samples were prepared in the pellets from 8 g of crushed sand with 4.5 ml of a compacted Elvacite resin.

The grain morphologies of S_T and S_B sands and the elaborated glasses are determined by means of a Scanning Electron Microscope ME03, SEM: Merlin, Zeiss, Cist. It allows maximum resolution of the secondary electron (SE) image from 0.8 nm at 15 KV, from 1.4 nm at 1 kV and from 2.4 nm at 0.2 kV. It also allows backscattered electron (BSE) imaging. The range of potential acceleration is between 0.02 V and 30 kV. SEM is coupled to the Energy Dispersive X-ray Spectroscopy (EDX) which provides information on the chemical compositions of sands and elaborate glasses.

The chemical composition of the glasses is determined by Electron Probe Micro-Analyzer (EPMA, CAMPARIS, Paris, France) with a CAMECA SX-Five apparatus equipped with five Wavelength- Dispersive X-ray Spectrometers (WDSs), driven by the Peak Sight software under Windows environment. Analyses are made with 15 kV accelerating voltage and a 10 nA sample current a 4 μm spot size. The standards for calibration were albite for Na, diopside for Mg, Si and Ca, Orthoclase for Al and K, $MnTiO_3$ for Ti, Cr_2O_3 for Cr, Fe_2O_3 for Fe and Cu for Cu. 20 points were taken and obtained compositions were averaged. Glasses Composition of glasses was homogeneous according EPMA. The samples were immobilized in an MECA PREX acrylic resin. The shots containing the glasses are then polished, cleaned and metalized.

The optical absorption spectra of the obtained glasses were realized with a double beam Perkin-Elmer 1050 spectrometer, in transmission mode. It scans a range of wavelengths between 300 and 4000 nm. The samples were previously polished with diamond paste. The optical absorption spectra were normalized by the samples thickness.

The color measurements of the samples were carried out by an X-Rite spectrometer, model 962 S/N 000967 (USA), X-Rite ink formulation software Pinter Pro 5.11 operating with D65 light source, camera viewing angle 10°. The measurements were repeated three times for each composition and an average value was taken. The samples thickness was 2 mm.

Knoop hardness measurements were carried out using a Zwick/Roel (ZHV) micro hardness tester. The load used in the hardness tests was 0.2 KP (1.9613 N) and the dwell time of the indenter in contact with the sample was 20 s.

Chemical resistance to acids and alkaline solutions of the samples were determined using chemical durability tests [21]. The samples are immersed in beakers filled with 1 N HCl or 1 N NaOH sample and then boiled for 6 h for HCl and 3 h for NaOH. The glasses are then washed with distilled water and dried at 105 °C for 24 h and their losses in weight are calculated. The glasses were also subjected to HF attack. A drop of HF (10 N) is disposed on the glasses surface for 10 min. The glasses were washed, with distilled water and then dried at 105° C during 24 h. The losses in weight of the samples were determined [22].

Results and discussion

Characterization of sand

Mineralogical analysis

Mineralogical analysis using X-ray diffraction of S_B sand shows presence of quartz. Albite is also determined in the X-ray diffraction pattern (Fig. 2).

TGA/TDA

According to the TGA/DTA thermogram of S_B sand (Fig. 3), three endothermic peaks are observed. The first peak at 105 °C corresponds to dehydration or release of free water. The second peak at 573 °C corresponds to the polymorphic thermal transformation of quartz (quartz α to quartz β). A third peak at 803 °C corresponds to the decarbonation of calcite. Moreover, a large mass loss (1.5%) is noticed on the TGA diagram which corresponds to the decarbonation and the loss of CO_2.

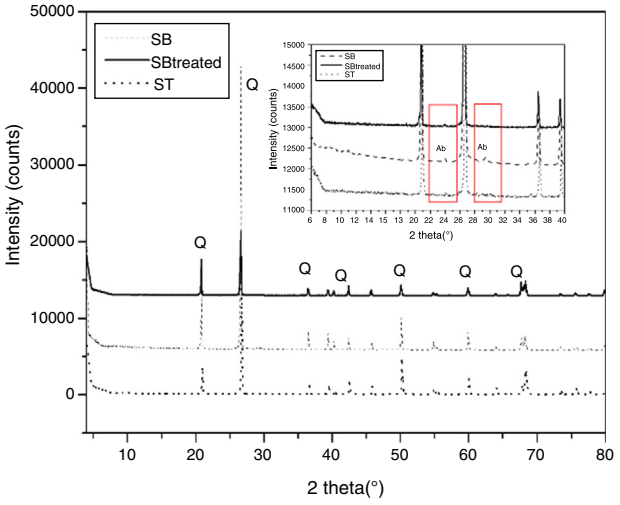

Fig. 2 – Diagram of X-Ray diffraction of S_T, S_B and S_B treated sands (Q: quartz, A: albite).

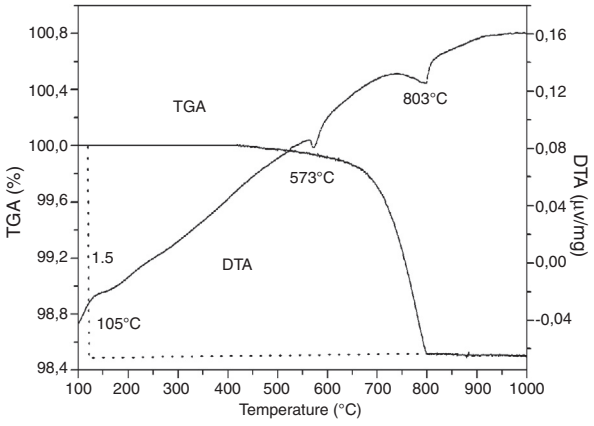

Fig. 3 – TGA/DTA thermogram of S_B sand.

Particle size distribution analysis

Sand with very fine grains is more likely to contain iron oxide and refractory minerals, while a large particle size causes fused inclusions in the final products, a phenomenon resulting from the slower melting of coarse grains in comparison with the finest [8]. Hence, the granulometric content of sands is a major requirement for glass manufacturers.

The laser granulometric analysis carried out by Coulter (Fig. 4) reveals that grains are formed by populations composed of 40 and 1000 μm sizes. It is also noticed that 50% of the grains in the sand are 243 μm in size. The particle sand size is fine but S_B sand meets the requirements of the glass industry (0.1–0.5 mm) [23]. Nevertheless, washing and sieving are necessary for the removal of the clay fraction.

Chemical composition

S_B is mainly composed of 95 wt% of SiO_2 (Table 2), Fe_2O_3 is present in a small amount (0.23 wt%), besides Al_2O_3 and TiO_2 (Table 2). In another hand, S_B contains clay fractions since its loss on ignition is 1.59%. These results are in concordance with the mineralogical and TGA/DTA analysis. In comparison with

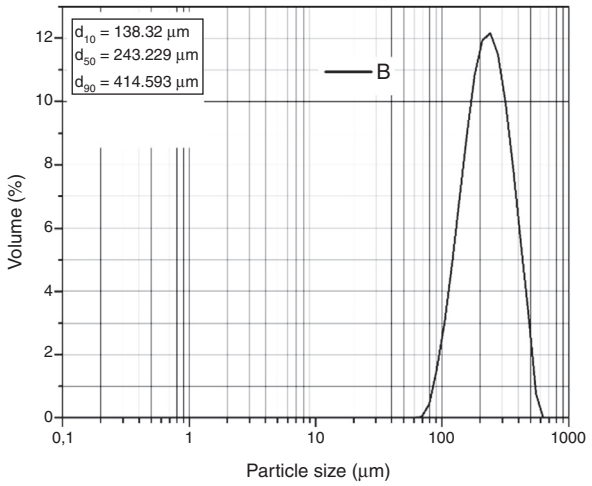

Fig. 4 – Particle size distribution of S_B sand.

the chemical composition of S_T, S_B contains more of Fe_2O_3 and less of SiO_2 and TiO_2 oxides (Table 2). The few amount of Fe_2O_3 content of the dolomite is additionally noticed.

Characterization of the treated sand

Mineralogical analysis

According to the X-ray diffraction patterns shown in Fig. 2, the samples of the two sands treated S_B and S_T have the same mineralogical composition, which consist of quartz. The disappearance of albite characteristic peak is also observed in the S_B treated sand.

SEM and EDX analysis

The SEM micrographs shown in Fig. 5 reveal that the quartz grains of the S_T Sand are ovoid in shape with marked surface asperities (i.e., roughness) indicating its belonging to fluvial origin. On the other hand, the quartz grains of S_B sand have a spherical and rounder form which characterizes the dune aeolian grains sand [24,25]. The Energy Dispersive X-ray Spectroscopy (EDX) attached to the SEM supports the XRF results concerning the same chemical elements contained in the two sands (Table 2).

Characterization and properties of the elaborated glasses

Chemical composition

Chemical analysis by electron microprobe (Fig. 6) shows that G_B glass presents the highest level of SiO_2, Na_2O, CaO, MgO, Al_2O_3 and Fe O, while G_T glass contains the highest level of K_2O and TiO_2. The high SiO_2 content in the G_B sample as compared to G_T is an indicator of the improvement in S_T quality. This improvement results from the treatment that it has undergone (washes and granulometric selection).

UV-Visible –IR Spectroscopy

As is shown in Fig. 7, the samples exhibit ordinary absorbance values for glasses. The UV cut-off in the absorption spectra was shifted to a higher wavelength from 325 nm to 350 nm for G_T and G_B samples, respectively. In the visible range

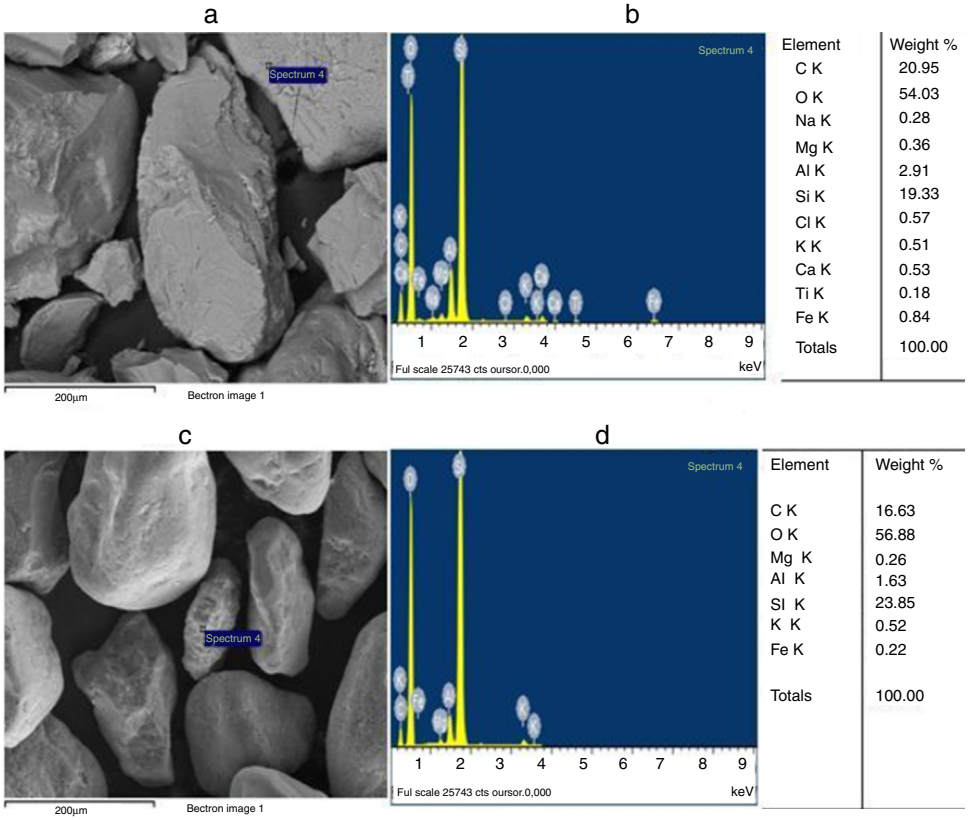

Fig. 5 – (a) SEM-SEI image of Tebessa sand particles, (b) EDX spectrum of Tebessa sand particle indicated in (a), (c) SEM-SEI image of Boussaâda sand particle, and (d) EDX spectrum of Boussaâda sand particle indicated in (c).

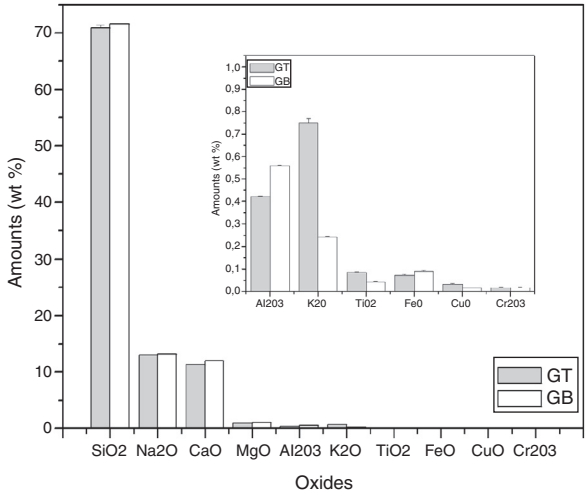

Fig. 6 – Chemical compositions of glasses.

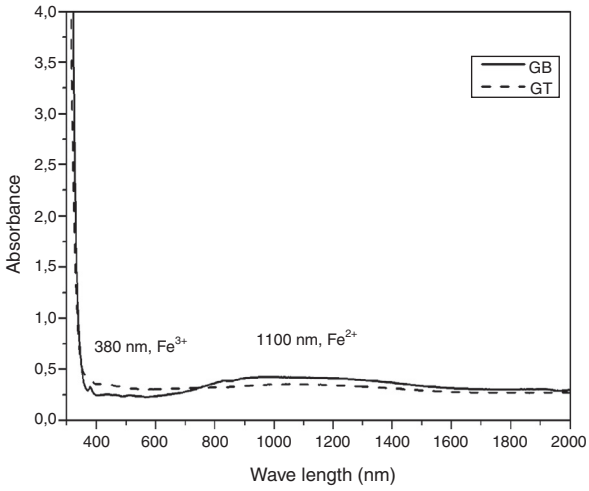

Fig. 7 – UV-Visible spectra of G_T and G_B glasses.

(400–800 nm), G_B has better transmission of light, compared with G_T. The spectra of two glasses present a peak at 380 nm characteristic of the Fe^{3+} ions charge transfer [11]. Beyond 800 nm, G_T has the best transmission. The appearance of a broad band centered at 1100 nm characteristic of Fe^{2+} ions in the G_B spectrum is also observed [11].

$L^*a^*b^*$ Color measures

According to Table 3, it is noticed that G_T is brighter and clearer than G_B with L^* values 91.96 and 87.67, respectively. G_B is also the most chromatic glass with $C = 2.21$. This is due to its higher contents of FeO and TiO_2 than G_T (0.09, 0.07 wt% of Fe O and 0.07, 0.04 wt% of TiO_2 for G_B and G_T, respectively).

The negative value of a^* parameter indicates a slight green color, which is mainly due to the presence of a mixture of

Table 3 – L*a*b * and C color parameters of G_T and G_B glasses.

Glass	L*	a*	b*	C
G_T	91.96	−1.41	−0.02	1.41
G_B	87.67	−1.32	−1.77	2.21
G_{B1}	88.62	−1.56	−1.29	2.02
G_{B2}	90.10	−1.47	−1.08	1.82
G_{B4}	90.50	−1.49	−1.05	1.82
G_{B6}	90.80	−1.37	−1.02	1.71
G_{B10}	91.05	−1.78	−0.48	1.84

Fe^{2+} and Fe^{3+} ions in the glass matrix. This value is negative as this mixture is high (case of G_B comparatively with G_T). However, the b* parameter is influenced by TiO_2 and Fe^{2+}/Fe^{3+} glasses amounts. The b* parameter of G_T present a value close to the characteristic of slight yellowish color. This result is due to the high proportion of Fe^{3+} in G_T glass than in G_B glass, this is in agreement with UV-Visible spectroscopy analysis. On the other hand, G_T contains more TiO_2 than G_B; this induces yellowish hue [26].

Knoop microhardness

As shown in Fig. 8, the Knoop microhardness values of the samples G_T and G_B are 465 and 451 HK respectively. The indentation hardness depends on the chemical composition of the glass, according to Scholze [27], addition of alkalis decreases hardness in silicate glasses. In fact, the content of Na_2O of G_B and G_T glasses are 13.24 and 13.03 wt% respectively whereas K_2O amounts are 0.24 and 0.75 wt% respectively. The highest microhardness value of G_T can be attributed to the highest amount of TiO_2 present in this glass comparatively with G_B glass (0.08 wt% and 0.04 wt% respectively) [10].

Improvement of the glasses properties

SEM and EDX analysis

The SEM observations illustrated in Fig. 9, reveals that G_{B0} and G_{B2} present a vitreous matrix free of bubbles and inclusions. Without TiO_2 addition, the glass exhibits a homogeneous morphology with a more or less compact vitreous network. In contrast, the glass resulted from 0.2 wt% of TiO_2 addition is more compact. The EDX Spectroscopy attached to the SEM report the presence of Ti and Fe in G_{B2} sample.

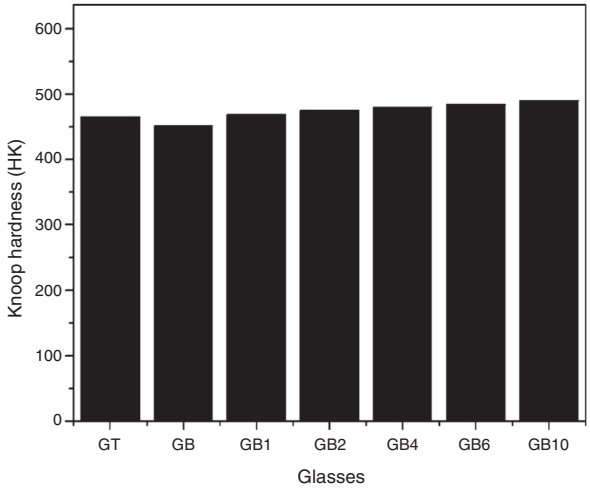

Fig. 8 – Knoop hardness values for the elaborated of glass.

UV-Visible-IR Spectroscopy

In general, the developed glasses absorption spectra in the UV-Visible near IR region (Fig. 10) have similar profiles. With the TiO_2 additions, the UV cutoff in the absorption spectra, showing an infinite ultraviolet absorption and a zero emission, was shifted to a higher wavelength from 350 nm to 370 nm. Similar results were obtained by Kumar [28]. A decrease in light transmission by the doped glasses, in the visible range, was additionally noticed. TiO_2 additions also influence the broad band around 1100 nm characteristic of Fe^{2+} ions (Fig. 10) [11]. A decrease in intensity of this broad band in the G_{B1} spectrum was noticed. Indicating a decrease in the level of ferrous ions in the G_{B1} composition compared with the other glasses. Characteristic absorption bands of the Ti^{3+} ions at 480–510 nm, 570 and 680 nm are not detected. These results are expected as under ordinary melting conditions, and it is difficult to obtain reduced Ti^{3+} ions in soda-lime silicate glasses [29]. TiO_2 addition also contributes to the increase in intensity of the peak at 380 nm, characteristic of the Fe^{3+} ions charge transfer [11] and the peaks at 430 and 480 nm, characteristic of the Fe^{3+} ions. According to the studies of the iron-doped glasses by Rus et al. [30] and Kukkadapu et al. [31], Fe^{3+} ions present absorption bands in the range 325–450 nm and 350–500 nm, respectively.

*L*a*b* Color properties*

According to Table 3, the glass G_B with no addition of TiO_2 is the most chromatic glass (C * = 2.21), by adding a small amount of TiO_2 (0.1, 0.2, 0.4 and 0.6 wt%), the chromaticity decreases to 1.71. Increasing the TiO_2 content to 1 wt%, the glass becomes more chromatic but still less than the G_B glass. The addition of TiO_2 increases the parameter b*, approaching the positive values characteristic of yellowish color. However, the values of the parameter a* are strongly influenced by the interference between Fe^{2+}/Fe^{3+} and Ti^{3+}/Ti^{4+} [26]. Its negative values indicate a slight green color attributed to the mixture of Fe^{2+} and Fe^{3+} ions. The TiO_2 addition brings an improvement in the glasses clarity represented by the L * parameter from 87.67 to 91.05 for G_B and G_{B10}, respectively.

Knoop micro hardness

As shown in Fig. 10, TiO_2 addition improves Knoop micro hardness of S_B based glasses. An increase of ~8.65 wt% of Knoop micro hardness is noticed for G_{B10} (with 1 wt% of TiO_2) comparatively with G_B. These results confirm the TiO_2 effect as an oxide influencing this mechanical property found in the case of G_B and G_T glasses. TiO_2 addition reinforces the glass network and produces an increase in the obtained glasses density [10], thus resulting in an increase in micro hardness for glasses containing TiO_2.

Chemical durability of the elaborated glasses

HCl and NaOH

The chemical durability tests in HCl (1 N) and NaOH (1 N) solutions showed (Fig. 11) that the glass samples are more durable in acidic solution than alkali ones. Thus, in acidic solution, G_B

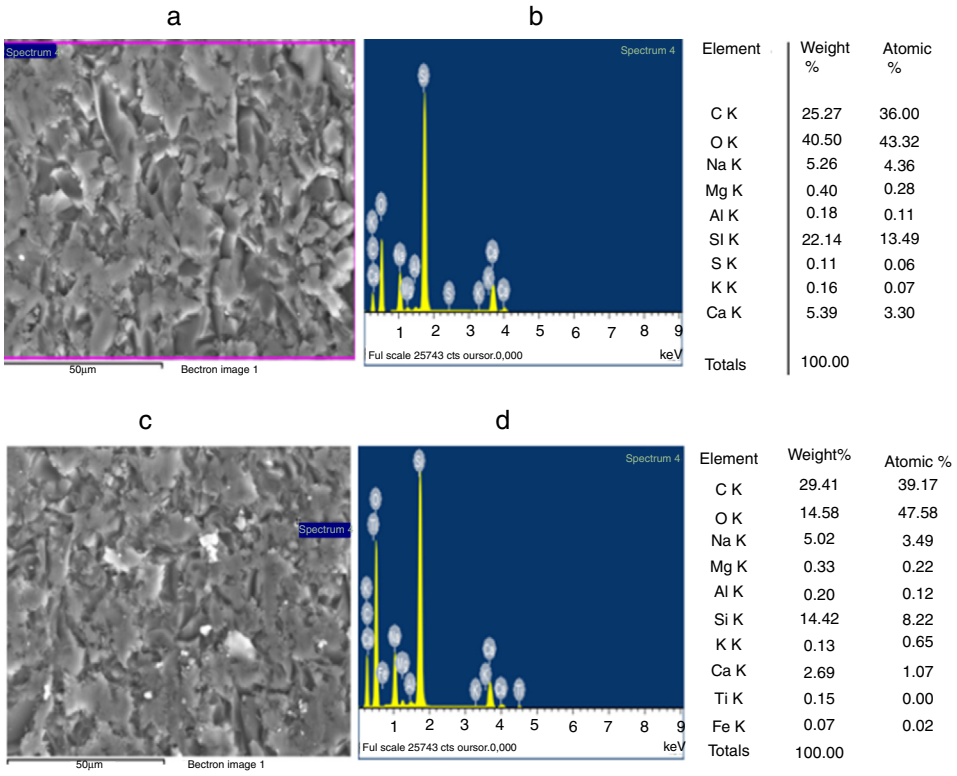

Fig. 9 – (a) SEM-SEI image G_{B0} glass, (b) EDX spectrum of G_{B0} glass indicated in (a), (c) SEM-SEI image of G_{B2} glass and (d) EDX spectrum of G_{B2} glass indicated in (c).

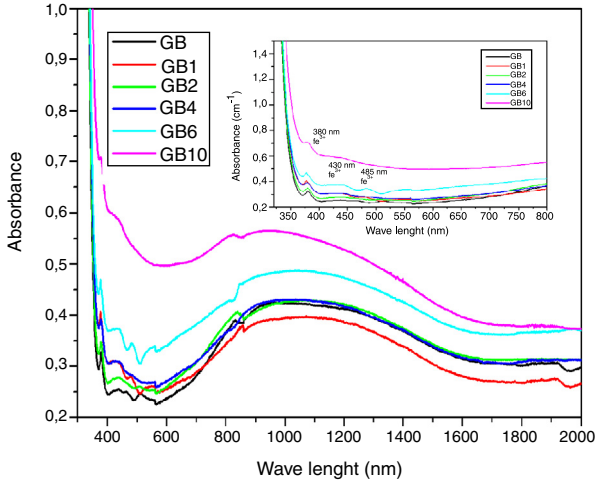

Fig. 10 – UV-Visible spectra of G_B with TiO_2 addition glasses.

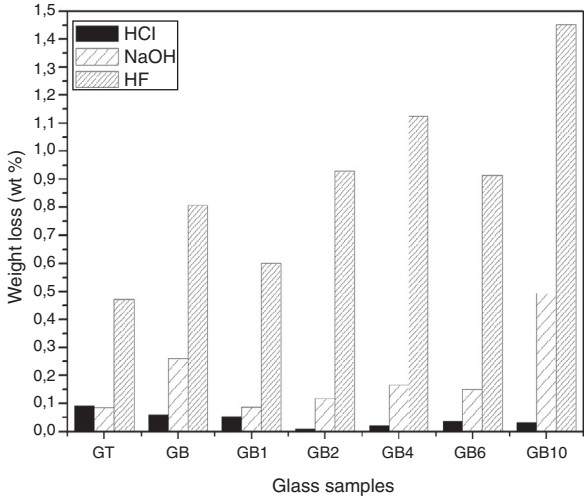

Fig. 11 – Weight loss (wt%) of the studied glasses by various solutions.

resists better, while it is more vulnerable in the presence of alkaline solution comparatively with G_T.

The addition of TiO_2 in G_B glass improves its chemical durability with respect to the HCl acid by reinforcing the vitreous network. However, in NaOH solution, the improvement is also observed except in the case of G_{B10} composition (1 wt% of TiO_2). Similar observations have been reported by El-Batal et al. [32] for the G_{B1} sample. The exception related to G_{B10} composition is due to the fact that Si–O–Si bonds are influenced by the addition of 1 wt% of TiO_2. It makes their breakdown by the hydroxyl ions (OH^-) contained in the alkaline solution easier. The incorporation of this TiO_2 amount in the glass network may increase the substitution of Si^{4+} by the Ti^{4+} ion with its larger ionic radius than that of Si^{4+} (0.061 and 0.040 nm, respectively) and thus increase the exchange engaged between the two ions [33].

Durability of the glasses in HF

The study of chemical durability in HF (10 N) for the developed glasses (Fig. 11) revealed that the vitreous network of the G_T sample is more resistant to attack than that of the G_B sample. This is related to the higher silica content of G_B compared to G_T.

The S_B sand glass compositions prepared with TiO_2 addition are more attacked by HF than the basic composition without TiO_2 addition. The variation of glass composition modifies the glass structure, leading to changes in the concentration of fragile bonds. An exception is noticed in the case of G_{B1} (with addition of 0.1 wt% of TiO_2) where an improvement in its durability is observed (with a mass loss of 0.602 compared to 0.807 and 0.472 wt% for G_B and G_T, respectively).

Conclusions

The physico-chemical characterization of the Boussaâda sand revealed the presence of a fraction with a particle size <100 μm carrying the ferrous impurity, thus requiring prior treatment before its use in the glasses elaboration. After the physical treatments by several washes and a granulometric selection, the characterization of S_B by X-ray diffraction revealed the disappearance of the clay fraction (albite and calcite).

The soda-lime glass produced from the Boussaâda sand is colorless, has an interesting light transmission that is better than the Tebessa sand glass and has a better chemical durability in acid solution (HCL solution (1 N)).

TiO_2 additions to S_B-based glasses have enhanced the clarity and transparency from $L^* = 87.67$ to $L^* = 91.05$ and improved the Knoop microhardness from 451 HK to 490 HK for G_B and G_{B10}, respectively. This improvement is due to the fact that TiO_2 affect on the Fe^{3+}/Fe^{2+} ions equilibrium in the vitreous matrix.

The glass chemical durability to attack by acid (HCl) and alkaline (NaOH) solutions is enhanced by the addition of TiO_2 amounts. However, the chemical resistance to attack by HF is enhanced only in the case of G_{B1} composition (with 0.1 wt% TiO_2).

The dune sand of Boussaâda is promising for its use as a raw material for the elaboration of glasses. Moreover, the addition of TiO_2 improves its colorimetric and mechanical properties besides its chemical durability in acids (HCl, HF) and alkaline (NaOH) solutions.

REFERENCES

[1] A. Benyoub, Le sable siliceux en Algérie, Portail Algérien des énergies renouvelables, Algérie, 2011.

[2] M.L. Mechri, S. Chichi, N. Mahdadi, S. Beddiaf, Diagnosis of the heating effect on the electrical resistivity of Ouargla (Algeria) dunes sand using XRD patterns and FTIR spectra, J. Afr. Earth Sci. 125 (2017) 18–26.

[3] L. Zeghichi, Z. Benghazi, L. Baali, The effect of the kind of sands and additions on the mechanical behavior of S.C.C, Phys Procedia 55 (2014) 485–492.

[4] Y. Abadou, R. Mittiche-Kettab, A. Ghrieb, Ceramic waste influence on dune sand mortar performance, Constr. Build. Mater. 125 (2016) 703–713.

[5] K. Arroudj, M. Ould Ahme, M.L. lanez, M.N. Oudjit, Caractérisation des mortiers à base des fines du quartz, 8 eme séminaire technique de Lafarge., Algérie, 2011.

[6] H. Meradi, L. Atouib, L. Bahloula, K. Boubendiraa, A. Bouazdiaa, F. Ismail, Characterization by thermal analysis of natural kieselguhr and sand for industrial application, Energy Procedia 74 (2015) 1282–1288.

[7] S. Platias, K.I. Vatalis, G. Charalampides, Suitability of quartz sands for different industrial applications, Procedia Econ. Financ. 14 (2014) 491–498.

[8] S. EM, A.B.B. Khairul, A.R. Sheikh, O.F. Radzali, B. Takahashi Phat, Comparison of silica sand properties from Kandalprovince, Cambodia and Tapah Perak, Malaysia, and characterization of soda lime silicate glass produced from Cambodian silica sand, Adv, Mater. Res. 858 (2014) 248–253.

[9] J.M. Fernández Navarro, Características de las materias primas para fusión de diferentes tipos de vidrios, Bol. Soc. Esp. Ceram. Vidr. 28 (1989) 449–459.

[10] E. Meechoowas, U. Pantulap, T. Jiwatchrakomal, Investigation of the properties of Soda- lime Silicate Glass Doped with TiO_2, Adv. Mater. Res. 979 (2014) 128–131.

[11] B. Mirhadi, B. Mehdikhani, Effect of batch melting temperature and raw materials on iron Redox state in sodium silicate glasses, J. Korean Ceram. Soc. 48 2 (2011) 117–120.

[12] J. Suba, D. Styriakova, Iron minerals removal from different quartz sands, Procedia Earth Planet. Sci. 15 (2015) 849–854.

[13] I. Styriakova, A. Bekenyiova, D. Styriakova, K. Jablonovska, I. Styriak, Second pilot-plant bioleaching verification of the iron removal from quartz sands, Procedia Earth Planet. Sci. 15 (2015) 861–865.

[14] N. Ay, E. Arica, Refining Istanbul's Silica Sand, Am. Ceram. Soc. Bull. 79 (2000) 89–91.

[15] Y. Kowada, H. Adachi, M. Tatsumisago, T. Minami, Electronic states of transition metal ions in silicate glasses, J. Non Cryst Solids 193 (1995) 316–320.

[16] R. Gwinn, P.C. Hess, Iron and titanium solution properties in peraluminous and peralkaline rhyolitic liquids, Contrib. Mineral. Petrol. 101 (1989) 326–338.

[17] J.E. Dickinson, P.C. Hess, Rutile solubility and titanium coordination in silicate melts Geo-chimica and Cosmos-chimica Acta. 49 (1985) 2289–2296.

[18] J. Zarzycki, Les verres et l'état vitreux, Masson, Paris, 1982.

[19] C. Fredericci, H.N. Yoshimura, A.L. Molisani, H. Fellegara, Effect of TiO_2 addition on the chemical durability of Bi_2O_3–SiO_2–ZnO–B_2O_3glass system, J. Non Cryst Solids 354 (2008) 4777–4785.

[20] M. Pouget, Les relations sol-végétation dans les steppes Sud-Algérois, Orostom, Paris, 1982.

[21] M.C. Vitorge, Durabilité chimique des verres, Dunod, Paris, 1992.

[22] T. Tomohiro, T. Yoshihiro, K. Yoshikazu, O. Kiyoshi, Preparation and properties of CaO-MgO-Al_2O_3-SiO_2 glass ceramics from Kaolin clay refining waste (Kira) and dolomite, Ceram Int. 30 (6) (2004) 983–989.

[23] J. Grolier, A. Fernandez, M. Hucher, J. Riss, Les propriétés physiques des roches: Théories et modèles, Masson, Paris, 1991.

[24] G.P. Padmakumar, K. Srinivas, K.V. Uday, K.R. Iyer, K. Pankaj Pathak, S.M. Keshava, D.N.D.N. Singh, Characterization of aeolian sands from Indian desert, Eng Geol 38 (49) (2012) 139–140.

[25] P. Vangala, M.L. Gali, Effect of particle size of sand and surface asperities of reinforcement on their interface shear behaviour, Geotext. Geomembr. 44 (2016) 254–268.

[26] N. Bouzidi, S. Aissou, N. Concha-Lozano, P. Gaudon, G. Janin, L. Mahtout, D. Merabet, Effect of chemico-mineralogical

composition on color of natural and calcined kaolins, Color Res. Appl. 39 (2014) 499–505.
[27] H. Scholze, Glass Nature, in: Structure and Properties, Springer-Verlag, New York, 1991.
[28] M. Kumar, A. Uniyal, A.P.S. Chauhan, S.P. Singh, Optical absorption and fluorescent behaviour of titanium ions in silicate glasses, Bull. Mater. Sci. 26 (3) (2003) 335–341.
[29] F.H. El-Batal, UV-visible, infrared, Raman and ESR spectra of gamma irradiated TiO_2- doped soda lime phosphate glasses, Indian J. Pure Appl. Phys. 47 (2009) 631–642.
[30] L. Rus, S. Rada, V. Rednic, E. Culea, M. Rada, A. Bot, N. Aldea, T. Rusu, Structural and optical properties of the lead based glasses containing iron (III) oxide, J. Non Cryst Solids. 402 (2014) 111–115.
[31] R.K. Kukkadapu, H. Li, G.L. Smith, J.D. Crum, J.S. Jeoung, W.H. Poisl, M.C. Weinberg, Mossbauer and optical spectroscopic study of temperature and redox effects on iron local environments in Fe-doped (0.5 mol% Fe_2O_3) 18 Na_2O-75 SiO_2, J. Non Cryst Solids. 317 (2003) 301–318.
[32] F.H. El-Batal, E.M. Khalil, Y.M. Hamdy, H.M. Zidan, M.S. Aziz, A.M. Abdelghani, FTIR spectral analysis of corrosion mechanisms in soda lime silica glasses doped with transition metal oxides, Silicon 2 (2010) 41–47.
[33] B. Mysen, P. Richet, Silicate Glass and Melts—Properties and Structure, Elsevier, 2005.